ACS Photonics

pubs.acs.org/journal/apchd5

Perspective

Empowering Metasurfaces with Inverse Design: Principles and Applications

Zhaoyi Li,* Raphaël Pestourie, Zin Lin, Steven G. Johnson, and Federico Capasso*

Cite This: https://doi.org/10.1021/acsphotonics.1c01850

Read Online

ACCESS | Metrics & More | Article Recommendations

ABSTRACT: Conventional human-driven methods face limitations in designing complex functional metasurfaces. Inverse design is poised to empower metasurface research by embracing fast-growing artificial intelligence. In recent years, many research efforts have been devoted to enriching inverse design principles and applications. In this perspective, we review most commonly used metasurface inverse design strategies including topology optimization, evolutionary optimization, and machine learning techniques. We elaborate on their concepts and working principles, as well as examples of their implementations. We also discuss two emerging research trends: scaling up inverse design for large-area aperiodic metasurfaces and end-to-end inverse design that co-optimizes photonic hardware and post-image processing. Furthermore, recent demonstrations of inverse-designed metasurfaces showing great potential in real-world applications are highlighted. Finally, we discuss challenges in future inverse design advancement, suggest potential research directions, and outlook opportunities for implementing inverse design in nonlocal metasurfaces, reconfigurable metasurfaces, quantum optics, and nonlinear metasurfaces.

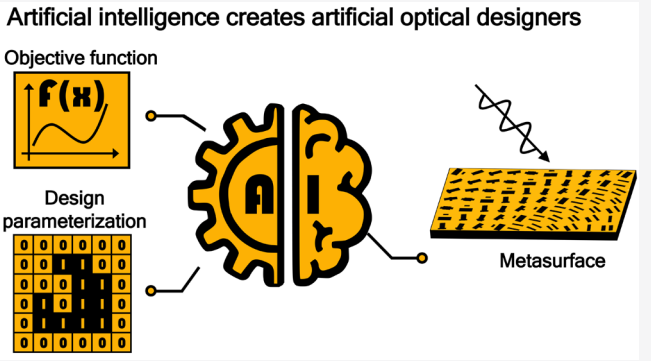

KEYWORDS: *metasurfaces inverse design, topology optimization, evolutionary optimization, machine learning, large-scale optimization, end-to-end optimization*

INTRODUCTION

The success of metasurfaces in the past decade is driven by the advancement of numerical simulation tools, material platforms, and fabrication techniques.[1−3] Metasurfaces exploited light-matter interactions to engineer wavefront at subwavelength resolution by using artificial meta-atoms. They not only unveil the rich physics of electromagnetic waves but also enable numerous functional devices that have technological implications, such as light detection and ranging (LiDAR),[4] compact spectrometers,[5−7] advanced cameras,[8−10] displays,[11] virtual/augmented reality systems,[12,13] etc. The working principle of metasurfaces is governed by Huygens' principle:[1] meta-atoms act as scatters or truncated waveguides[14,15] to generate secondary wavelets that mutually interfere. Inspired by that, most metasurface design so far utilizes a first-principle forward strategy like "phase matching". One needs to first deduce an analytical solution of a targeted phase profile relying on physical intuition and then seek to match it with a predefined meta-library. Such a design strategy works well for a device with simple functionality like a focusing lens for a single wavelength. Unfortunately, in many cases one may face the following situations where the conventional forward design is less useful or even not applicable: the target phase profiles cannot be numerically solved, the solutions cannot be satisfied by a meta-library, the solutions are not unique, etc. As the device functionality complexity, design constraints, and design degrees of freedom scale up, the future success of metasurfaces demands an innovation in design philosophy.

Inverse design emerges as a disruptive strategy to tackle the bottlenecks of metasurface design.[16−22] Fundamentally different from forward design methods, inverse design is method agnostic and aims to solve a physics problem by utilizing a mathematical tool. It formulates the device functionality as an objective function and performs an optimization task that can be subject to constraints. There are many advantages when using inverse design: First, it is well suitable for a metasurface with complex functionality that cannot be solved analytically. Second, it is method agnostic and does not need *a priori* knowledge of physical principles. Third, it can be powered by many advanced computational algorithms, especially the recent blooming of artificial intelligence. Fourth, it allows searching in

Received: December 2, 2021
Revised: May 3, 2022
Accepted: May 3, 2022

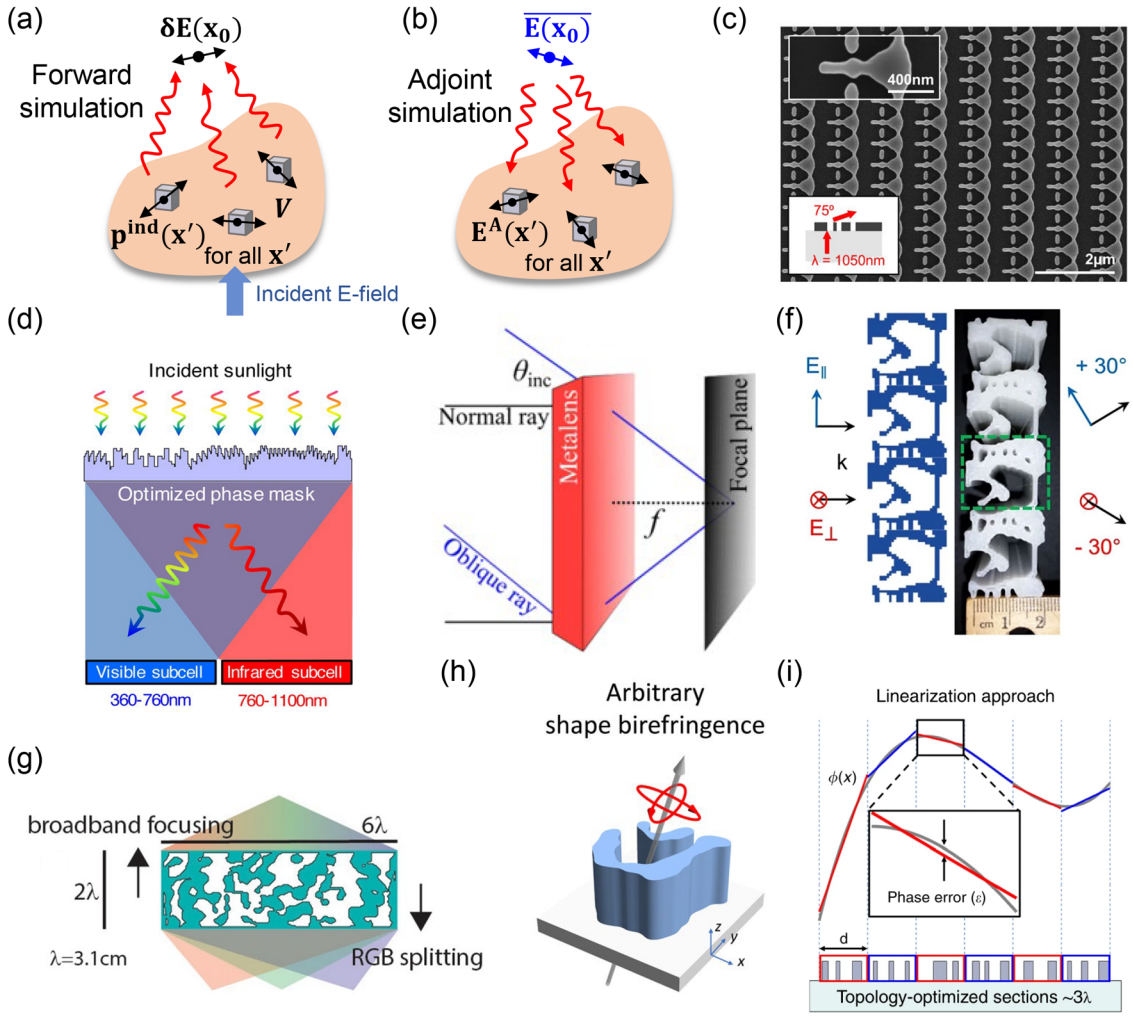

Figure 1. Metasurface inverse design based on topological optimization. (a) Schematic of a forward simulation to compute the change of electric field due to material permittivity perturbation. (b) Schematic of an adjoint method to compute adjoint field that is driven by an artificial electric dipole deduced from the forward simulation. (c) Scanning electron microscopy image of a meta-grating. Reprinted with permission from ref 29. Copyright (2017) American Chemical Society. (d) Schematic of a diffractive element that splits the solar spectrum into two spectral bands directing to separated partitions in the far field. Reprinted with permission from ref 31. Copyright (2016) American Chemical Society. (e) Schematic of a multilayered 2D metalens concentrator that focuses oblique incidence to a single spot. Reprinted with permission from ref 33. Copyright (2018) by the American Physical Society. (f) An inverse-designed 3D-printed polarization splitter working at 33 GHz. Reprinted with permission from ref 35. Copyright (2018) The Author(s) https://creativecommons.org/licenses/by/4.0/. (g) Schematic of a device that realizes broadband focusing and RGB spectral splitting depending on the direction of incident beam. Reprinted with permission from ref 36. Copyright (2021) The Author(s) https://creativecommons.org/licenses/by/4.0/. (h) Schematic of a freeform meta-atom that exhibits angle-dependent shape birefringence. Reprinted from ref 38. Copyright (2020) The Author(s), some rights reserved, exclusive AAAS. Distributed under a CC BY-NC 4.0 license https://creativecommons.org/licenses/by-nc/4.0/. (i) Schematic of a 2D metalens consisting of topologically optimized segments. Reprinted with permission from ref 39. Copyright (2019) The Author(s) https://creativecommons.org/licenses/by/4.0/.

a full design space and finding nonintuitive solutions with optimal performance. Fifth, it is a powerful tool for optimizing multifunctional metasurfaces. It systematically searches for a balance among intercoupled physical parameters, like phase vs amplitude, and enables quantitative trade-offs between multiple wavelength/polarization/depth/angle-dependent goals. Cross-talks among multifunctionalities can also be considered and minimized. More importantly, inverse design can help unveil new physics phenomena and offer new physics insights.

METASURFACE INVERSE DESIGN METHODS

Topology Optimization. Topology optimization aims to determine an optimal structural layout using a mathematical tool. In the past decades, it has demonstrated success in solving industrial problems ranging from designing stiffener ribs for aircraft to lightweight mechanical parts for vehicles. Recently, it became an important tool for nanophotonic inverse design.

A key feature of topology optimization (TO) is a large degree of design freedoms that lead to nearly arbitrary shapes. A typical TO formulation considers every pixel or voxel in the design region as a design variable, often leading to 10^3–10^9 degrees of freedom. In particular, the design space is discretized into pixels or voxels, each of which contains a continuous design variable characterizing materials property. For example, the design variable α for a binary dielectric nanophotonic device can be related to the dielectric profile:

$$\varepsilon(\vec{r}) = (\varepsilon_2 - \varepsilon_1)\alpha(\vec{r}) + \varepsilon_1$$

https://doi.org/10.1021/acsphotonics.1c01850
ACS Photonics XXXX, XXX, XXX−XXX

where ε_1 and ε_2 denote the permittivity of two materials, r is the spatial location, and $\alpha \in [0,1]$ is the design field. $\alpha(\vec{r})$ may be initialized to a constant (a uniform state) or a random distribution (a grayscale state). During optimization, perturbative modifications are gradually added to $\alpha(\vec{r})$ iteratively until a satisfactory solution is obtained. Meanwhile, a threshold projection filter[16,23−25] is applied to enforce the material permittivity being either ε_1 or ε_2.

The possible solutions in a high-dimensional design space are enormous, and gradients of the merit function with respect to design variables are needed for efficient optimization convergence. The gradients provide directional guidance to the optimizer to improve the merit function. Fortunately, it is possible to compute the gradient for each design variable efficiently using an adjoint method. One only needs to perform a forward simulation and an adjoint simulation to obtain all gradients at once.[26−28] Without losing generality, the merit function can be written as $F(E) = \int f(E(x))\, d^3x$, where $E(x)$ is the vectorial electric field in the observation domain, and F is the merit function. A perturbation in material permittivity ε change at location x' in the device domain induces polarization $p^{\text{ind}}(x') = \alpha V E(x')$, where α denotes the polarizability, and V is the volume of perturbation. The corresponding change in merit function can be computed as $\delta F = 2V\text{Re}[\alpha E(x')\cdot E^A(x')]$, where Re denotes real part, and $E^A(x')$ is the field in the device domain from the adjoint simulation using an artificial electric dipole with amplitude $\partial f/\partial E(x)$ at the observation plane. For example, the merit function of a single wavelength metalens optimization can be formulated as $F = \frac{1}{2}|E(x_0)|^2$, where $E(x_0)$ is the electric field at the design focal spot. The change F due to the permittivity perturbation at x' can be expressed as $\delta F = \text{Re}[\overline{E(x_0)} G(x_0, x') p^{\text{ind}}(x')]$, where the overline denotes complex conjugation, and $G(x_0,x')$ is the Green's function that tells the electric field change at x_0 due to dipole of unit amplitude at x' (i.e., $\delta E(x_0) = G(x_0,x')p^{\text{ind}}(x')$ (Figure 1(a))). Due to the symmetry of Green's function and Lorentz reciprocity, the merit function change can be rearranged as $\delta F = \text{Re}[G(x', x_0)\overline{E(x_0)} p^{\text{ind}}(x')]$, and the first term represents the adjoint electric field at x' by dipole with amplitude of $\overline{E(x_0)}$ (i.e., $E^A(x') = G(x', x_0)\overline{E(x_0)}$ (Figure 1(b))). This formula indicates δF for every position x' can be known by using only a forward (Figure 1(a)) and an adjoint simulation (Figure 1(b)): $\delta F = \text{Re}[E^A(x')p^{\text{ind}}(x')]$.

An early application of topology optimization in nanophotonics reshapes the design of dielectric waveguides and photonic crystals.[16] We refer the readers to comprehensive reviews[23−25] on topology optimization for a broad view. Here, we focus on the recent implementation of topology optimization in metasurface inverse design. One of the earliest examples of topology-optimized metasurface is demonstrated by Sell et al.[29] In this work (Figure 1(c)), the author showed a meta-grating based on freeform geometries for beam deflecting. The deflection efficiency is significantly larger than conventional designs based on forward approaches especially at high deflection angles. The inverse-designed meta-device achieves ∼75% absolute deflection efficiency for both TE and TM polarizations at a wavelength of 1050 nm. The metasurface supported multiple Bloch modes, which were engineered in a nonintuitive way by topology optimization. Similarly, Xu et al. demonstrated a catenary-like metasurface using topology optimization for wide-angle and high-efficiency deflection.[30]

The topology optimization enables multifunctional metasurface inverse design by formulating a composite objective function. Xiao et al. demonstrated a diffractive spectral-splitter that spatially separated the visible and near-infrared bands of sunlight (Figure 1(d)).[31] The inverse design objective function is a sum of T_{VIS} and T_{IR}, which denote the averaged transmission coefficient through subcells that collect visible and infrared light, respectively. Sell et al. demonstrated a multiwavelength meta-grating splitter using a discrete wavelength-multiplexed objective function.[32]

Multilayered metasurfaces and even three-dimensional metamaterials can be designed using topology optimization. Lin et al. showed a topology optimized multilayered 2D cylindrical metalens that corrects the off-axis aberration at a set of discrete angles of incidence ranging from −20 degrees to 20 degrees (Figure 1(e)).[33] In another work, a multilayered 2D metalens concentrator that can focus light with 11 different angles of incidence to a single focal spot was designed.[34] Such device functionality is barely possible by using a single-layered metasurface. Callewaert et al. demonstrated an inverse-designed 3D-printed meta-device that splits light depending on polarization at microwave frequency (Figure 1(f)).[35] A reconfigurable 3D-printed meta-device has been demonstrated by Ballew et al. by using topology optimization (Figure 1(g)).[36] This device realizes RGB color sorting and focusing by mechanical switching. In addition, Christiansen et al. showed that the topology optimization can be even applied to design multiscale multiwavelength metalenses.[37] The authors demonstrated a multilayered axi-symmetric metalens that has a tunable focal length at a wavelength of 10 μm by changing the material index and another device that focuses light at both wavelengths of 1 and 10 μm.

There are significant advantages in using topology optimization in metasurface design: First, it can find nonintuitive device layouts that are not accessible by traditional forward methods, Second, it can help explore nonintuitive new device physics. For example, Shi et al. demonstrated a topological-optimized metasurface that realizes angle-dependent birefringence (Figure 1(h)).[38] Third, it can greatly improve the performance of metasurfaces by exploring larger design domain (Figure 1(i)).[29,39−41] Fourth, it can consider device performance robustness against fabrication errors.[42] More generally, several methods have been devised that can ensure robust fabricability for topology-optimized designs.[43,44]

While there are many merits to topology optimization in inverse design, questions and challenges remain to be resolved in the future. First, since TO takes advantage of gradient-based local optimization methods, it is not guaranteed to find true global optima for most problems of interest which are nonconvex (i.e., the design space contains local minima/maxima). However, if the design space is sufficiently large for a given merit function and constraints, the optimization landscape typically involves a large of number of local optima with comparable performance to the global optimum so that TO can efficiently settle into one of these "good" solutions—a well-known observation in the theory of optimization known as "blessing of dimensionality".[45,46] In fact, the "hardest" optimization problems are known to be those where the design space may be large but barely large enough for a desired functionality. For such problems, sophisticated search strategies in addition to local gradient descent may be required

https://doi.org/10.1021/acsphotonics.1c01850
ACS Photonics XXXX, XXX, XXX−XXX

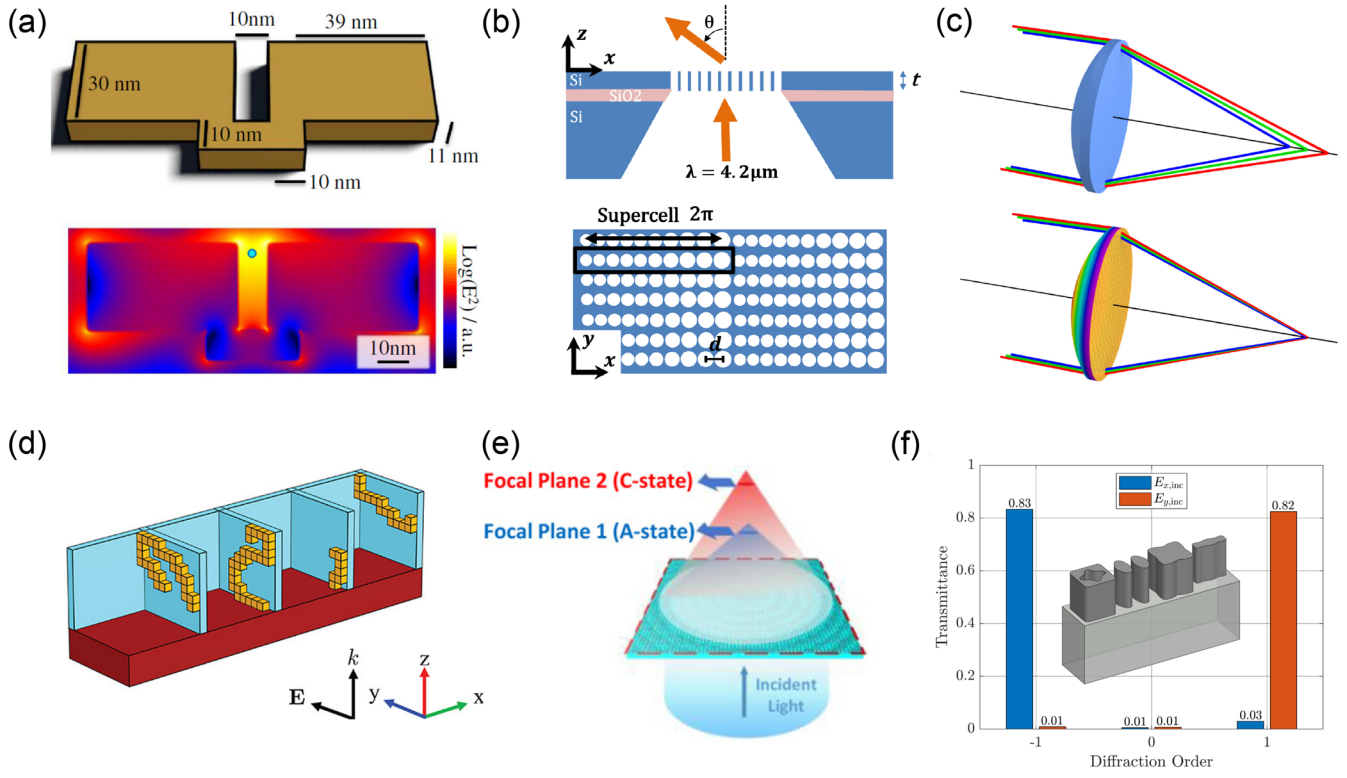

Figure 2. Metasurface inverse design based on evolutionary optimization. (a) Schematic of a split-ring antenna designed using a genetic algorithm and simulations of its near field intensity distribution. Reprinted with permission from ref 53. Copyright (2012) The American Physical Society. (b) Schematic of a beam deflector metasurface consisting of a nanohole array. The structure is designed using particle swarm optimization. Reprinted with permission from ref 62. Copyright (2017) The Optical Society. (c) Comparison between a chromatic homogeneous lens and an apochromatic metasurface-GRIN lens using a covariance matrix adaptation evolutionary strategy. Reprinted with permission from ref 64. Copyright (2018) The Optical Society. (d) Schematic of a 3D metasurface supercell using a multiobjective lazy ant colony optimization. Reprinted with permission from ref 71. Copyright (2016) American Chemical Society. (e) Schematic of a varifocal metalens based on phase-change material that can be designed using a multiobjective optimizer. Reprinted with permission from ref 72. Copyright (2020) The Author(s) https://creativecommons.org/licenses/by/4.0/. (f) Schematic of a silicon metasurface supercell based on freeform meta-atoms using BORG optimizer. Reprinted with permission from ref 73. Copyright (2020) The Optical Society.

(such as multistart algorithms[47] or deterministic global optimization[48]). For a certain class of problems involving at most quadratic functions of electromagnetic fields, useful insights about the nature of global optima may be obtained by using recently developed Lagrange-dual frameworks to compute shape-independent bounds on light-matter interactions.[49−52] However, it remains an open challenge to extend these frameworks to problems involving general nonquadratic merit functions. Second, most of the topology optimization so far consumes considerable computation power when using Maxwell equation solvers like FDTD or FEM methods. Thus, it is difficult to scale up the aperiodic metasurface topology optimization to millimeter or centimeter sizes.

Evolutionary Optimization. Evolutionary optimization (EA) is a generic population-based numerical optimization algorithm, which emulates the behaviors of biological systems. It belongs to global optimization techniques that attempt to find a global optimal solution as opposed to local optimizers and does not use gradient information. In this section, we illustrate several EA techniques that are widely used in a metasurface inverse design problem.

Genetic algorithm (GA) is a well-known example. It encodes potential solutions in a chromosome-like data structure and uses iterative evolution to generate an optimal solution. There are three key phases during evolution: first, data selection by choosing better designs as parents for the next generation; second, crossover that recombines pairs of breeders to increase population; third, mutation that modifies parts of chromosomes to maintain genetic diversity. GA is a suitable method for combinatory inverse design problems that have discrete sets of solutions.[17,18] Feichtner et al. optimized the near-field enhancement of plasmonic antennas using a GA (Figure 2(a)).[53] It shows an improvement by a factor of 2 compared with a reference nanorod antenna. Sui et al. deployed a GA-based topology inverse design method to demonstrate an ultrawideband polarization conversion metasurface.[54] The metasurface features pixelated structures with different symmetries. Cai et al. implemented an inverse design of a transmissive focusing metalens considering nonlocal interaction by a GA-based optimization.[55]

In addition, many modified versions of GA have also been demonstrated. Jafar-Zanjani et al. demonstrated an adaptive genitive algorithm in designing a binary plasmonic reflect array for beam-steering.[56] This method includes a flow of objective function updates such that the optimization first converges to a set of solutions satisfying high-priority subobjectives and then improves the other low-objective subobjectives. Li et al. implemented a microgenetic algorithm for design of broadband infrared metasurface absorbers. Compared with a conventional GA, it initiates with a much smaller population

https://doi.org/10.1021/acsphotonics.1c01850
ACS Photonics XXXX, XXX, XXX−XXX

and converges faster.[57] Jin et al. introduced a hierarchical evolutionary algorithm to design meta-hologram.[58] This optimization begins in a lower segmentation of the device with a coarse resolution and evolves to higher segmentation with high resolution.

Ant-colony optimization (ACO) is another type of EA algorithm. It is inspired by ants' foraging social behavior of seeking a path between their colony and source food. It was widely used in finding an optimal solution to a dynamic graphic problem, like the traveling salesman problem.[59] In the field of metasurface design, ACO is suitable to find a continuous structure for a combinatorial problem. Lewis et al. applied ACO in the design of a meander line antenna with high efficiency at a microwave frequency.[60]

Particle swarm optimization (PSO) was developed by imitating the social behavior observed in flocks or schools of birds. The optimization starts with a population of particles with random initialization. These particles search for a global optimum by acting both independently and cooperatively. The position update of each individual particle during optimization iterations depends on its momentum, the best personal position, and the best global position of the group. In the end, the particles converge to a common best position representing a global optimum. Different from GA and ACO, a PSO can be applied to solve a continuous design problem whose solution is a vector of real numbers instead of binary values. Kildishev et al. designed a negative-index-metamaterial design using PSO.[61] Ong et al. combined a gradient descent technique and PSO to design a freestanding nanohole array metasurface for optimized beam deflection efficiency (Figure 2(b)).[62]

Covariance matrix adaptation evolution strategy (CMA-ES) is self-adaptive and requires less user-defined parameters. It is also used in metasurface inverse design. Elsawy et al. explored CMA-ES in the design of cylindrical nanopillars arrays that achieve 85% deflection efficiency for both TM and TE polarizations and at a wavelength of 600 nm.[63] Nagar et al. used CMA-ES to design a hybrid apochromatic lens consisting of a gradient-index lens and a metasurface working in the visible (Figure 2(c)).[64]

Other evolutionary algorithms have also been developed for metasurface inverse design including a simulated annealing method for the design of binary plasmonic structures that engineer surface plasmon polaritons,[65] A branch-and-bound method for a true global optimization of thin-film optical filter design,[66] a multi-island differential evolution for a metasurface color filter design,[67] and a Bayesian optimization method to search for a global optimal design of phase gradient metasurfaces,[63] etc.

The examples above show a single-objective optimization (SOO) strategy for an inverse design problem with a single objective function. When coming to a complicated design problem with multiple competing objectives, multiobjective optimization (MOO) is a more suitable tool. The idea of MOO derives from a concept of "Pareto optimality" in economics defining a high-efficiency state where no single improvement can be made without worsening the others.[68] MOO explores the "Pareto front" in the hyperdimensional design space that consists of a set of nondominated solutions. These solutions cannot be further simultaneously improved toward all objectives. The MOO has advantages over the SOO: (1) one does not need to manually prioritize the objective functions; (2) it shows trade-offs between objective functions; (3) it gives a set of solutions instead of a single solution by SOO. Wiecha et al. applied a GA-based MOO to design silicon antennas that can simultaneously achieve high scattering efficiency at a first wavelength for x polarized light and at a second wavelength for y polarized light.[69] Those silicon nanostructures were used to realize polarization-encoded microimages. Zhu et al. implemented a multiobjective lazy ant colony optimization algorithm (MOLACO) to design a three-dimensional frequency selective surface (FSS) (Figure 2(d)).[70] The FSS exhibits a design stop band at 6 GHz and pass band at 8 GHz with wide field of view. In another work, Zhu et al. also adapted MOLACO to design a three-dimensional phase-gradient plasmonic metasurface supercell that achieves 84% first-order diffraction efficiency at mid-infrared.[71] Shalaginov et al. designed a MOO-assisted reconfigurable metasurface design (Figure 2(e)) based on a phase change material $Ge_2Sb_2Se_4Te_1$(GSST).[72] Simulations show that the device deflects normal incident light to −1 diffraction order in the amorphous state and to 0 diffraction order in the crystalline state at a wavelength of 5.2 μm. Whiting et al. presented a BORG multiobjective evolutionary algorithm to generate a high-performance freeform meta-atom library.[73] The library is further used to build a multifunctional shape-optimized metasurface like a polarization-dependent beam splitter (Figure 2(f)).

Machine Learning. Machine learning aims to imitate the way that humans learn by performing tasks automatically through "experience" instead of being explicitly programmed. A deep neural network (DNN), a subfield of machine learning, is an algorithm that is inspired by biological neural networks in nature. Its recent development has impacted many fields including computer vision, speech recognition, drug discovery, genome sequencing, etc. In recent years, DNNs have driven the advancement of nanophotonics and metasurfaces research.[19,20,22] Here, we focus on how DNNs enhance metasurface inverse design.

The basic architecture of a DNN consists of layers of artificial neurons (mathematical operators) that are connected in series: from an input layer to an output layer through at least one hidden layer. Depending on the form of connection between neuron layers, there are different classes of DNNs. Here, we focus on two mostly used ones: multiplayer perception (MLP) and convolutional neural network (CNN). In a MLP, each neuron is a many-to-one data mapping operator that receives a data vector x from neurons in a previous layer and outputs a scalar y to a neuron in the next layer. The operation can be formulated as $y = f(w^T x + b)$, where w is a weight vector, b is a bias term. Both w and b are trainable through a learning process by iterations of forward propagations and backward propagations. f is a differentiable and nonlinear activation function. The nonlinearity of the activation is critical to neural network accuracy, and commonly used ones include sigmoid, hyperbolic tangent, rectified linear unit function, etc. CNNs are usually used in image-based data processing. In the two-dimensional case, the input data is in the form of a matrix that can contain image information. A kernel filter, consisting of a matrix of weight factors, is applied spatially over the input layer plane. At each position, the kernel passes a single output value to one neuron in its next layer. The operation of the kernel is similar as in MLP: a sum of product of weight matrix and input data matrix followed by an activation function. The kernel filters are designed to extract local spatial features from the input layer. More generally, each

https://doi.org/10.1021/acsphotonics.1c01850
ACS Photonics XXXX, XXX, XXX−XXX

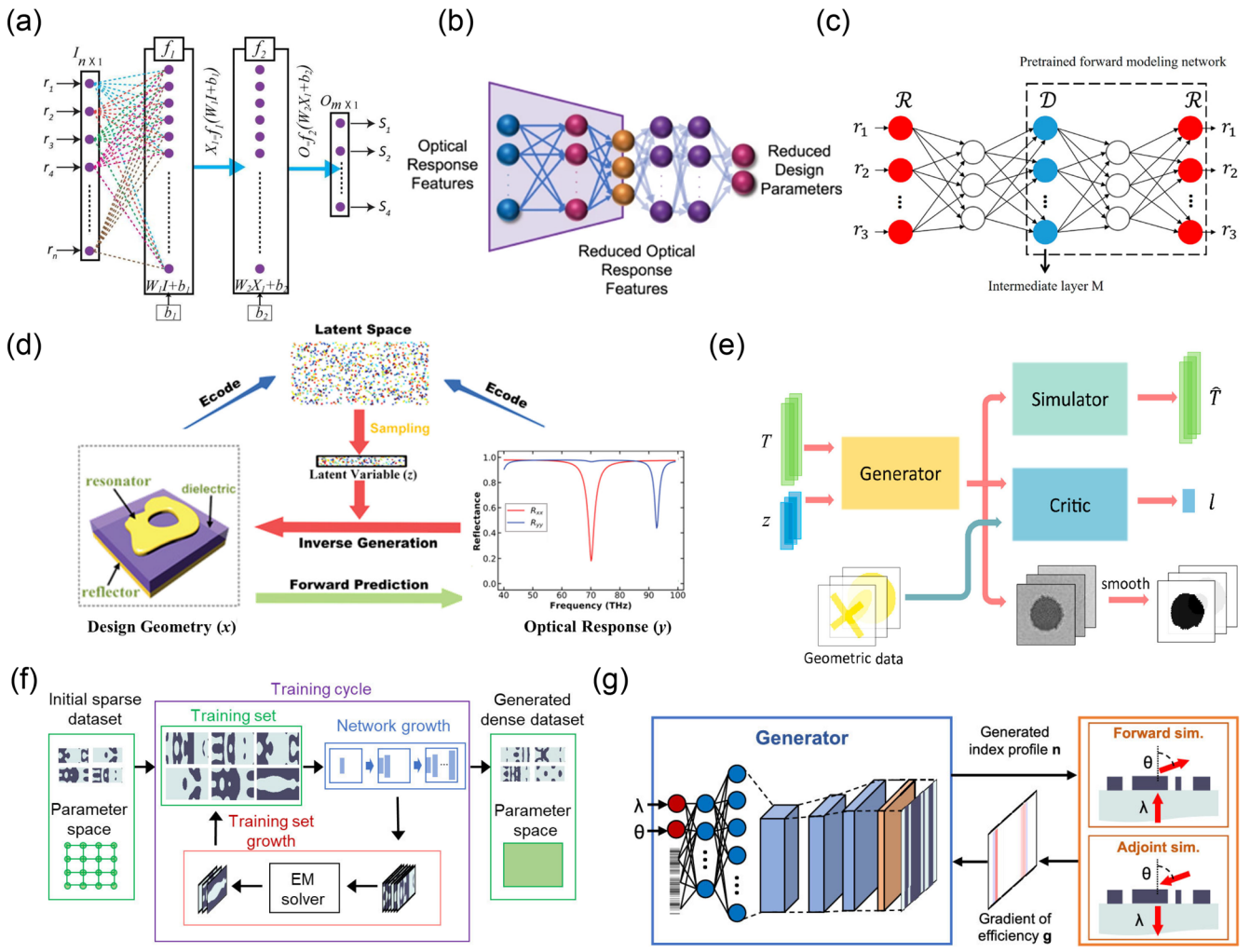

Figure 3. Metasurface inverse design based on machine learnings. (a) A deep neural network used to predict optical response of a metasurface given design parameters. Reproduced with permission from ref 75. Copyright (2018) American Chemical Society. (b) A backward deep neural network based on an autoencoder that maps from optical response space to design space. Reprinted with permission from ref 78. Copyright (2020) The Author(s) https://creativecommons.org/licenses/by/4.0/. (c) A bidirectional neural network consisting of a forward and a backward network for inverse design. Reprinted with permission from ref 82. Copyright (2018) American Chemical Society. (d) A generative deep neural network based on a variational autoencoder for metamaterial design and characterization. Adapted with permission from ref 86. Copyright (2019) Wiley-VCH Verlag GmbH & Co. KGaA, Weinheim. (e) A generative adversarial network that learns structure−property relationships and generates an optical spectrum form a metasurface (and vice versa). Reprinted with permission from ref 88. Copyright (2019) American Chemical Society. (f) A variation of generative adversarial network that is based on progressively growing networks architectures. Reprinted with permission from ref 91. Copyright (2020) American Chemical Society. (g) A generative neural work for global optimization of meta-gratings. Reprinted with permission from ref 93. Copyright (2019) American Chemical Society.

neuron layer can be represented as a tensor (stacked matrices) when it involves multiple kernel filters. The nature of complicated neuron connections in a DNN enables capturing complex nonlinear relationships between inputs and outputs and thus is a tool for regression and classification tasks.

A discriminative DNN is designed to discriminate between groups of data. Mathematically, it computes $argmax_y P(y|x)$, where x are training data, y is a label, and P is a probability function. It aims to predict the most likely y class considering x. Discriminative DNNs are used as surrogate models in replacement of numerical electromagnetic solvers. Given design variables x of a device, which can be physical geometries, material properties, wavelengths, or others, the DNN can predict (interpolate) its physical responses $y = f(x)$, where y can represent transmission/reflection spectra, electromagnetic fields, band structures, etc. It helps reduce computation time by orders of magnitude once the neural network has been fully trained. Sajedian et al. demonstrated a model to predict the absorption responses from plasmonic structure images by combining a CNN and a recurrent neural network.[74] The training set contains 100 K simulations with random structures. Deep learning is ∼35 times faster than simulations.

The fast DNN-based surrogate models in tandem with numerical optimization techniques open a pathway to metasurface inverse design. Inampudi et al. used an interior-point optimization method with a DNN (Figure 3(a)) to design metagratings for a desired diffraction efficiency distribution.[75] Nadell et al. developed a forward DNN model where the input is a metasurface geometry that comprises a supercell of four dielectric cylindrical resonators, and the output is its frequency-dependent transmittance spectra.[76] By

https://doi.org/10.1021/acsphotonics.1c01850
ACS Photonics XXXX, XXX, XXX−XXX

combining it with a developed "fast forward dictionary search" algorithm, they solved the inverse design problem of finding device candidates that match with designed spectra. Zhelyeznyakov et al. inverse designed a metasurface that focuses light at 633 nm and produces an annular beam at 400 nm.[77] The inverse design framework includes a DNN that accelerates the mapping the near field of cylindrical scatters and a gradient-descent optimizer. In addition, an autoencoder framework can further help reduce the dimensionality of the design space, which facilitates the numerical optimization process.[78] Liu et al. demonstrated a method to encode the binary image of a photonic nanostructure design into a sparse representation in the Fourier domain.[79]

A discriminative DNN can also work in an opposite way (Figure 3(b)) that directly searches for an optimal solution in device design space x given a device physical response y, i.e., $x = f(y)$. It is conceptually straightforward but difficult to execute because of the nonuniqueness nature of such a problem. It is not trivial to get such a neural network properly trained to converge to multiple solution branches. To mitigate this issue, Zhang et al. proposed a multibranched neural network inverse model.[80] This model automatically redirects contradictory information into different values and associates multiple outputs of physical parameters to a single input of electrical parameters. Lin et al. trained a CNN to design plasmonic metasurface comprising nanodiscs.[81] They artificially enforced a unique mapping from optical response to metasurface geometry by restricting the nanostructures symmetry during the data training process. Reducing data dimensionality using an autoencoder (i.e., an encoder combined with a decoder) is another strategy to overcome nonuniqueness issues. Kiarashinejad et al. used an autoencoder that reduces the dimensionality of both design space and response space.[78] It converts a many-to-one design problem to a one-to-one design problem.

A bidirectional DNN is another method to solve a metasurface inverse design problem.[82] It consists of both an inverse network and a direct network (Figure 3(c)). The inverse network predicts a device design x given an input of device response y, and the output x is then fed into the direct network to predict its device response y'. The training process aims to minimize the difference between y and y'. Malkiel et al. used a bidirectional DNN to design plasmonic structures for a targeted polarization-dependent optical response.[83] The DNN is composed of a geometry-predicting-network and a spectrum-predicting-network. It shows better accuracy than using inverse network only. Similarly, Mai et al. used a directional DNN approach to optimize chiral plasmonic metamaterials exhibiting strong circular dichroism response at mid-infrared region from 30 to 80 THz.[84] An et al. applied it to an all-dielectric meta-filter inverse design.[85]

A generative neural network is another class of DNNs. This network aims to learn a correlation between training data x and its respective label y by modeling $P(x,y)$, which is a joint probability distribution. It can then generate a new data set x' after learning, and that is why this model is called "generative". Its key difference from a discriminative neural network is that its input data resides in a latent space. The term "latent" means that variables z in this space have no explicit meaning but rather represent a probability distribution such that $P(z) = P(x|y)$. The latent variables z are fed into a generative neural network together with the label y and generate an output x' that $x' = f(z|y)$. Here, we highlight two main types of generative neural network, namely variant autoencoder (VAE) and generative adversarial network (GAN), which are widely used in metasurface inverse design.

A VAE comprises an encoder that maps input data to a distribution in the latent space and a decoder that maps a sampled variable from the distribution to generate new data. VAEs can generate device variants similar to the training set by learning from their principal features. It can also be used to generate a new distribution of devices with a parameter label interpolated from the training set. Ma et al. presented an inverse design strategy using a VAE network (Figure 3(d)).[86] The encoder takes device structure images and their corresponding optical responses as input and latent variable distributions as output. The decoder functions as a generative network that uses sampled latent variables with a targeted optical spectrum to generate new metasurface designs. In addition, it represents another solution to a one-to-many inverse design problem. VAE can also play together with a numerical optimizer for solving inverse design. Liu et al. combined a VAE and an evolutionary optimization method to search an optimal metasurface with an on-demand transmission spectra.[87] Here, the optimization algorithm acts on the latent variables that represent photonic design.

A GAN comprises a generative network and a discriminative network. It is a two-layer contest: on the one hand, the generator aims to generate new data instances that mimic training data and fool the discriminator. On the other hand, the discriminator tries to better differentiate the generative data from the training data. These two networks are trained together, and after training completion the generator can generate new data approximating the training data enough that the discriminator cannot tell their difference. Liu et al. showed an inverse design model based on GAN that generates plasmonic metasurface for targeted transmission spectra with customized resonances (Figure 3(e)).[88] The generator was trained to generate fake devices using inputs of a conditioned label of transmission spectra and latent variables. The discriminator was trained to learn the difference between real and fake samples and in turns guide the generator to produce samples with common features as training samples. The generator and discriminator work together to learn the structure−property relationship and generate new devices with a designed transmission behavior. An et al. used a GAN model to design multifunctional metasurfaces that exhibit polarization-dependent focusing.[89] The metasurfaces comprise meta-atoms that are produced by generator through learning a meta-atom library. Jiang et al. presented an inverse design method to generate freeform metagratings with high efficiency at a design deflection angle and wavelength.[90] This method is based on a GAN that learns topological optimized metagratings at a set of design wavelengths and deflection angles. Wen et al. further showed that a progressively growing generative network can produce devices with higher efficiency and robust performance (Figure 3(f)).[91] Similarly, Kudyshev et al. inverse designed thermal emitters with high efficiency by learning from topological optimized devices via an adversarial autoencoder network.[92] Finally, a hybrid inverse design method based on a GAN helps address the challenges of searching global-optimized device. Jiang et al. showed a global topological optimization network combining a GAN in tandem with an adjoint-based topological optimizer outperforms the topological optimizer alone (Figure 3(g)).[93]

https://doi.org/10.1021/acsphotonics.1c01850
ACS Photonics XXXX, XXX, XXX−XXX

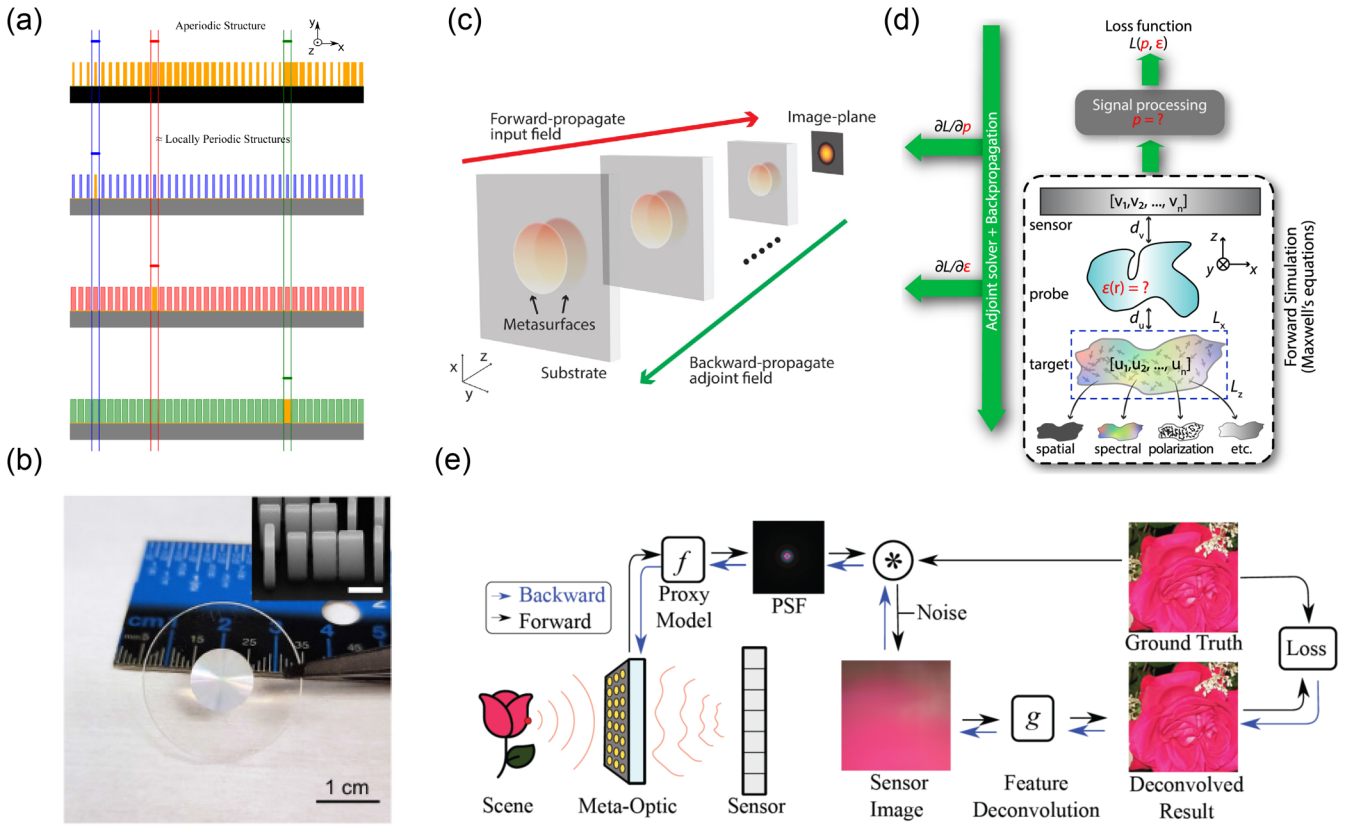

Figure 4. Large-area and end-to-end metasurface inverse design. (a) Schematic of local periodic approximation method that decomposes an arbitrary aperiodic metasurface into a set of periodic scattering problems. Reprinted with permission from ref 101. Copyright (2018) The Optical Society. (b) Photography of a 1 cm diameter RGB-achromatic metalens by using inverse design. Reprinted with permission from ref 105. Copyright (2020) The Author(s) https://creativecommons.org/licenses/by/4.0/. (c) An inverse design framework for cascaded metasurface optics. Reprinted with permission from ref 104. Copyright (2019) The Optical Society. (d) Schematic of an end-to-end inverse design framework that includes photonic design and signal processing design. Reprinted with permission from ref 111. Copyright (2020) The Author(s) https://creativecommons.org/licenses/by/4.0/. (e) An end-to-end inverse design framework that is based on convolutional neural networks. Reprinted with permission from ref 113. Copyright (2021) The Author(s) https://creativecommons.org/licenses/by/4.0/.

ML techniques have proven unique strengths in metasurface inverse design. However, their weakness cannot be ignored, and innovations are needed in future development. First, the required training data in ML sets scales up exponentially with the dimensionality of the design space.[20] Owing to that, ML is difficult to be applied to an inverse design of large-scale and complex devices. For example, a device consisting of 100 degrees of freedom may need a large training data quantity of up to 10^7. It is well-known as the "curse of dimensionality".[94,95] Many efforts have been attempted so far to reduce the large data dependence and increase the tractability of a complex inverse design problem including active learning,[96] transfer learning,[97] and physics-informed learning.[98,99] Second, ML is a data-driven technique in nature. It performs like a "black box" for data analysis without straightforward physical interpretation. The training difficulty arises because its accuracy and stability highly depend on the training set, and extensive hyperparameter tuning may also be required case by case. The lack of underlying physics understanding imposes another application bottleneck. For example, most ML-based metasurface inverse design so far is constrained to an individual unit cell of subwavelengths scale. When dealing with a large-scale metasurface consisting of complex aperiodic unit cells, the usefulness of ML techniques in harnessing the nonlocal light-matter interaction is questionable. Zhelyeznyakov et al. showed initial steps toward deep learning of a metasurface supercell consisting of multiple scatters.[77] In addition, S. An et al. used a neural network to predict the mutual coupling of meta-atoms.[100] Looking ahead, innovations are anticipated to enrich ML networks with valuable existing physics-based tools like transfer matrix and Fourier optics.

Emerging Trends in Metasurface Inverse Design. A major goal in artificial intelligent design of metasurfaces is finding a feasible solution to a large-scale optimization problem that contains thousands or even millions of design parameters. Increasing degrees of design freedom brings more possibilities in device solutions with better performance or new functionality. A large-scale metasurface is also demanding in a realistic application. However, searching for an optimal solution in a hyperdimensional design space is very difficult. One needs a fast and accurate electromagnetic modeling method replacing a brute-force Maxwell equation solver to evaluate the performance of a multiscale device in many optimization iterations. The scale of device size and feature size can be orders of magnitude apart. For example, a mm-scale metasurface can contain unit cells with a periodicity of hundreds of nanometers. A feasible pathway is to decompose a large simulation domain into smaller subdomains, which are computationally tractable. Multiple boundary conditions have been explored for the subdomains. The locally periodic

https://doi.org/10.1021/acsphotonics.1c01850
ACS Photonics XXXX, XXX, XXX−XXX

Table 1. Comparison between Forward Design and Inverse Design[a]

	forward design	inverse design
Methods	Physics-driven approach: phase matching method, etc.	Data-driven approaches: many computational algorithms including TO, EO, ML, etc.
Computational cost	Low computational cost (+)	Higher (method-dependent) computational cost (−)
	Easy to scale up (+)	Difficult to scale up (−)
Physics interpretation	Straightforward interpretation (+)	Less physics intuition (−)
Applicable design regime	Limited to simple device functionality (−)	Simple, complex or multiple device functionalities (+)
	Limited in considering design constraints (−)	Systematically consider design constraints (+)
Requirements of *a priori* knowledge	Needs explicit analytical solutions of EM fields everywhere (−)	Does not require a priori knowledge and inversely discovers solutions (+)
Other features	No feedback loops for performance evaluation (−)	Feedback loops for performance optimization (+)
	Optimizes EM fields by considering meta-atomss separately (−)	Optimizes EM fields by considering meta-atoms collectively (+)
	Limited in considering couplings between meta-atoms (−)	Can consider couplings between meta-atoms (+)
	Limited in addressing cross-talks among multifunctionalities (−)	Good at addressing cross-talks among multifunctionalities (+)

[a]TO stands for topological optimization, EO stands for evolutionary optimization, ML stands for machine learning, and EM stands for electromagnetic. (+) means advantage, and (−) means limitation.

approximation[101] assumes periodic boundary conditions (Figure 4(a)); however, it has been rigorously shown to break down for very oblique angles.[102] For subwavelength subdomains, coupling to neighboring subdomains can be taken into account using the local phase method;[103] however, this approach is computationally intensive. Other boundary conditions such as perfectly matched layers[39] and overlapping domains[40] supplement the locally periodic approximation for designs that require high numerical apertures and very oblique angles. Once the subdomains are defined, two approaches can be used to solve Maxwell's equations: either the equations are solved with a brute force solver as in topology optimization,[34] or Maxwell's equations are solved by calling a pretrained surrogate model that maps geometry parameters to complex transmission coefficients in shape optimization.[101] The former approach gives more degrees of freedom in the metasurface design, because every pixel can be a design degree of freedom, at the cost of more intensive computation. The latter approach is much faster; however, it is limited in the number of parameters for the subdomain because the cost of training the surrogate model increases significantly with the number of design degrees of freedom. The simplest surrogate is to construct a library which matches a single parameter per subdomain to a local response as Backer et al. designed cascaded systems of metasurfaces (Figure 4(c)).[104] For two to five parameters, Chebyshev interpolation is a very efficient surrogate;[101] however, the need for training data goes exponentially with the number of degrees of freedom. Recently, Li et al. demonstrated a centimeter-scale inverse-designed meta-optics (Figure 4(b)) using this type of surrogate.[105] The aperiodic meta-optics contains ∼ a billion unit cells and shows wavelength- and polarization-dependent functionalities. For example, the authors demonstrated metalenses that show polarization-insensitive RGB-achromatic focusing and polychromatic focusing by employing anisotropic nanofin structures. These experiments demonstrate the significance of inverse design in the regime of high-dimensional parameter space and complex device functions. Similarly, Bayati et al. demonstrated a 1 mm-diameter meta-optics with extended depth of focus by using an inverse design framework.[106] For more design parameters in the surrogate model, machine learning techniques have been recently developed for data efficiency and applied to large scale optimization.[96,107] The global trend for both topology and shape optimization is to add more physical degrees of freedom to the design by increasing the scale of the devices, enabling a more complex scattering with subdomains bigger than the wavelength, and exploring more physical geometry parametrizations.

One can simulate metasurfaces entirely and more accurately based on Mie scattering theory and transfer matrices; however, it is currently limited to subdomains with ellipsoid features and without substrate.[108,109] The inverse design is performed on the whole structure and computationally expensive. More recently, a GPU-accelerated full-Maxwell solver can simulate metasurface of 100 × 100 λ^2 within 5 min.[110] Another approach to large-scale metasurface optimization is combining forward and inverse design methods. Li et al. showed a hybrid method for RGB-achromatic meta-optics design.[13] The meta-optics of 2 mm diameter is judiciously divided into multiple zones. A forward design approach is applied to engineer dispersion of each individual zone, and an inverse design approach is applied to engineer the interference among zones.

Recent research efforts added parameters from image postprocessing to the optical device parameters for end-to-end inverse design. Computer vision has reshaped information acquisition from images by taking advantage of advanced computational algorithms. Conventional computer vision emphasizes software advancement for imaging processing at the back end, with little attention paid to the development of optics hardware at front. On the one hand, most imaging systems for computer vision rely on geometric optics, which is not only bulky but also limited in understanding the wave nature of light like its polarization or spectral information without using filters. On the other hand, metasurfaces exploit wave physics via light-matter interaction at subwavelength resolution. They enable compact and aberration-free imaging systems. However, most meta-imaging systems directly map an object onto an image sensor without involving computational postprocessing.

The marriage between metasurfaces and computer vision opens up a new artificial intelligent imaging paradigm. The end-to-end metasurface inverse design aims to optimize the optics front end in conjunction with computation-imaging

https://doi.org/10.1021/acsphotonics.1c01850
ACS Photonics XXXX, XXX, XXX−XXX

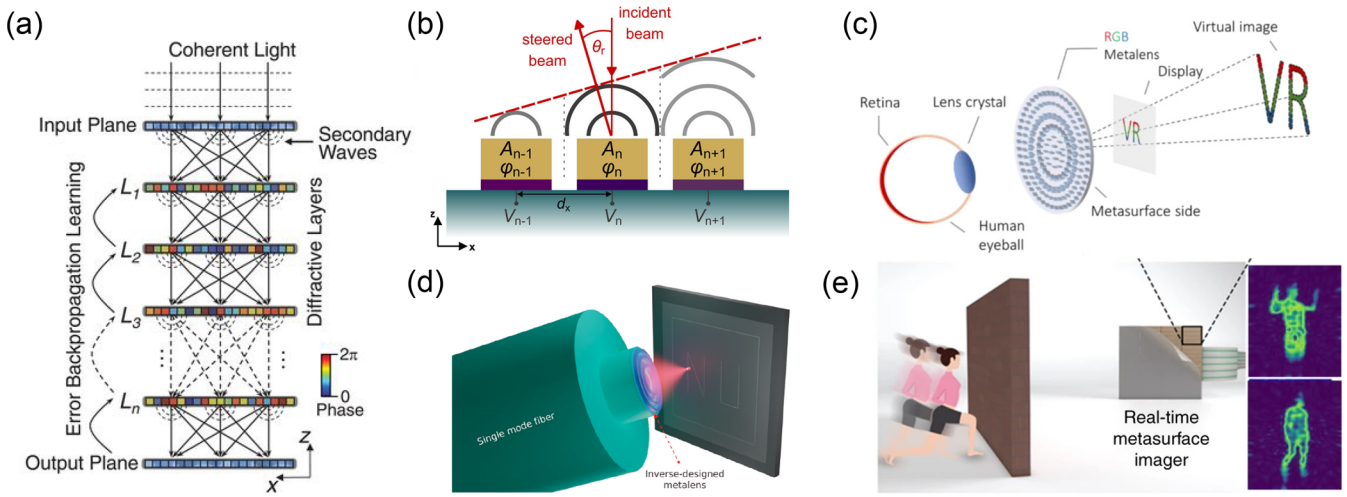

Figure 5. Applications of inverse-designed metasurfaces. (a) Schematic of a diffractive neural network comprising multiple transmissive layers that performs at the speed of light. Reprinted with permission from ref 114. Copyright (2018) AAAS. (b) Schematic of a beam steering active metasurface based on plasmonic antennas and ITO. Reprinted with permission from ref 115. Copyright (2020) American Chemical Society. (c) Schematic of a compact virtual reality platform based on an RGB-achromatic meta-eyepiece. Reprinted from ref 13. Copyright (2021) The Author(s), some rights reserved, exclusive AAAS. Distributed under a CC BY-NC 4.0 license https://creativecommons.org/licenses/by-nc/4.0/. (d) Schematic of inverse designed metalens 3D-printed on an optical fiber tip that is used for direct laser lithography. Reprinted with permission from ref 117. Copyright (2021) American Chemical Society. (e) Schematic of a programmable metasurface imager that detects body gestures. Reprinted with permission from ref 118. Copyright (2019) The Author(s) https://creativecommons.org/licenses/by/4.0/.

back end. It empowers computer vision with rich physics and new capabilities in data acquisition. Lin et al. showed an end-to-end inverse design framework (Figure 4(d)) for a meta-imaging system that can extract spatial, spectral, and polarization information simultaneously in a single shot without any filter.[111] The metasurface comprises multiple layers of freeform nanostructures with spatially varying height. The image postprocessing algorithm is Tikhonov (L_2) regularization method.[112] The nanostructure design variables (height) and the regularization parameters in the computational algorithm are co-optimized. A general objective function in an end-to-end problem is the loss function $L(\varepsilon,p) = \langle \|u - \hat{u}\|^2 \rangle_{u,\eta}$, where ε is the metasurface design parameter, p is the algorithm parameter, u is the ground-truth image, is the reconstructed image, η is the noise, and $\langle ... \rangle_{u,\eta}$ denotes the average over many u and η. The gradients of the objective function L with respect to p and ε is obtained by a backpropagation method and an adjoint method. The design framework seeks optimal ε and p that minimizes the loss function. In another work, Tseng et al. included a feature-based imaging postprocessing based on a convolution neural network (Figure 4(e)).[113] The neural network performs image deconvolution using extracted image features instead of raw image intensity. The end-to-end inverse design chain co-optimizes meta-optics and the neural network. The author showed examples of high-quality reconstructed images by an inverse-designed meta-imager in tandem with a trained imaging algorithm.

In the end, we compare forward design and inverse design from aspects including methods, computational cost, physics interpretation, applicable design regime, requirements of *a priori* knowledge, and other features. Table 1 summarizes the details highlighting both their advantages (+) and limitations (−). In general, inverse design is superior to forward design in many aspects but still has challenges to be addressed in future research.

Applications of Inverse-Designed Metasurfaces. Besides applications in design of a high-performance optical component like lenses, gratings, filters, beam splitters, and exploration of new phenomena like angle-dependent birefringence as discussed above, inverse designed metasurfaces have an impact in many other areas. Here, we summarize examples of recent works. Lin et al. demonstrated an all-optical machine learning platform, called D^2NN, using a stack of 3D-printed inverse-designed diffractive surfaces.[114] The D^2NN is an optical analogy of a classic computer-based neural network (Figure 5(a)). It operates based on the Huygens' principle, and each point in the diffractive surface functions as an artificial neuron that generates secondary waves. The transmission/reflection coefficient of each point is a learnable network parameter, which is iteratively adjusted through training. The D^2NN can implement complex functions like a classifier for digits/images at the speed of light. Zhan et al. demonstrated an array of inverse-designed Mie scatterers that can shape the light focus in three dimensions, for example, a depth-variant discrete helical pattern.[109] It can be potentially used in a depth-camera. Thureja et al. demonstrated an active beam steering metasurface (Figure 5(b)) by using an inverse design approach.[115] Though the deployed antennas are nonideal because it does not cover the full 2π phase range with unity transmission amplitude, the inverse design strategy offers nonintuitive array designs that enable high-directivity beam steering. Furthermore, the required phase modulation range for high beam directivity can be as low as 180°. The demonstrated design method for a nonideal active metasurfaces may have significant impact in light detection and ranging (LiDAR), holographic displays, etc. In another work, Chung et al. showed an inverse designed metasurface based on liquid crystal that realizes wide deflection angle and high switching efficiency.[116] Li et al. demonstrated the potential impact of inverse-designed meta-optics in the field of virtual reality and augmented reality (Figure 5(c)).[13] By using an

https://doi.org/10.1021/acsphotonics.1c01850
ACS Photonics XXXX, XXX, XXX−XXX

inverse design tool in conjunction with dispersion engineering, it is possible to harness light interference at different wavelengths both locally and nonlocally and realize RGB-achromatic focusing. The design principle defies the conventional understanding of physical constraints governing a Fresnel lens. It also addresses a major challenge of traditional optical lenses, that form factor and chromatic aberrations are hard to reduce at the same time. A next-generation VR platform was demonstrated by combining a meta-optics and a miniaturized fiber scanning display. In a recent work, Li et al. demonstrated an inverse design framework that is well suited for a large-scale (cm-scale) metasurface optimization problem.[105] The combination of large-aperture meta-optics and a laser back-illuminated micro-LCD opens a new path to compact and high-resolution VR imaging. Hadibrata et al. demonstrated an application of inverse-designed metasurfaces in fiber optics and optical lithography (Figure 5(d)). An inverse-designed metalens was fabricated on an optical fiber tip via a 3D direct laser-writing technique.[117] The fiber-tip lens was implemented as an objective in a homemade two-photon laser-writing setup, which achieved a feature writing size of ~200 nm. Li et al. recently demonstrated that a dynamic metasurface-imager (Figure 5(e)), which is controlled by a machine-learning assisted programming technique, realized real-time body imaging and body gesture classification.[118] It opens a new paradigm for intelligent surveillance, compressed sensing, and beyond.

DISCUSSION AND OUTLOOK

Inverse design has greatly reshaped the landscape of metasurfaces research. Looking ahead, inverse design anticipates unlocking even greater possibilities by using more geometrical and physical degrees of freedom. More geometrical freedom can be introduced by considering larger subdomains and volumetric (or multilayer) designs. Richer scattering effects that result from increased geometrical freedoms and dimensions are key to the next paradigm shift in inverse design inspiring a new generation of metasurface platforms. What is more, inverse design is essential in reducing the modeling errors of metasurfaces by considering multilayer or near-field couplings,[100] which are neglected in forward design methods. So far, it is still a challenging task and requires innovations to realize the inverse design of large-area, volumetric, and freeform metasurfaces especially considering the computational cost and fabrication complexity. With further development of inverse design techniques, we envision that inverse-designed freeform meta-atoms[73] and supercells[119] will enable high-performance, large-scale metasurfaces with higher efficiency, broader spectral bandwidth, wider angular bandwidth, and better dispersion/polarization control in the near future.

Even richer physics can be realized by incorporating novel material properties/effects into the inverse design formulation. For example, a majority of existing metasurface designs can be characterized as "local" in the sense that the incident electric field is transformed by the "local" scattering coefficients restricted to each unit cell—very often, a single transmission coefficient in the case of a subwavelength unit cell. We expect that much more comprehensive models using larger unit cells, simulating angle-sensitive scattering in Fourier space, and/or taking into account nearest-neighbor couplings will enable richer "non-local" effects and stronger spatial dispersion. More generally, exotic media with arbitrary angle-dependent permittivity $\varepsilon(k)$ (for example, photonic crystal superprisms[120] and nonlocal meta-materials[121,122]) may be inverse-designed in conjunction with a local metasurface, of which the computation is more tractable, to achieve enhanced sensitivities and unprecedented functionalities such as non-paraxial imaging, space squeezing, and hyperfine depth sensing.

Inverse design can also have impacts on the development of reconfigurable metasurfaces[123−125] integrated with active materials that possess dynamic device functions in response to external stimuli like electric/magnetic tuning, optical tuning, mechanical tuning, thermal tuning, etc. Despite different tuning mechanisms, a common research interest in this field is to optimize a device's multiple functions in different dynamical states. In such a case, inverse design presents a powerful tool to systematically balance among multiple objectives, evaluate device performance trade-offs, as well as reduce their cross-talks. Similarly, it can be applied to design time-varying metasurfaces with spatiotemporal light control.[126]

Another exciting direction for metasurface inverse design is to incorporate quantum models in various forms and contexts. For example, in imaging domains, quantum illumination protocols have enabled enhanced detection capabilities in noisy environments as well as ultra-Rayleigh subdiffraction resolutions.[127−129] On the other hand, metasurfaces can also be used to greatly influence the coherence and entanglement of quantum objects (such as qubits).[130] We envision that an end-to-end inverse-design formulation of quantum meta-optics (classical Maxwell photonics combined with quantum design) will serve as a springboard for launching a new era of quantum engineering technologies.

Nonlinear optics is another rich area of metasurface research that presents a wide range of applications from signal processing, optical switching to biosensing.[131] Metasurfaces can exhibit a strong nonlinear optical response by electromagnetic field localization and enhancement.[132] In addition, they can relax phase-matching constraints[133,134] and offer unprecedented control over polarization and spin−orbital coupling.[135] Inverse design paves a way to study the relationship between metasurface topology and light−matter interactions in nonlinear regime, providing valuable insights to further improve frequency conversion efficiency. Benefiting from enhanced nonlinearity, a nonreciprocal metasurface can break the time-reversal symmetry of wave propagation.[136,137] It is a promising candidate to realize light isolation over THz bandwidth. With the help of inverse design, nonreciprocal wave propagation is expected to occur at lower light intensity and over a broader bandwidth.

AUTHOR INFORMATION

Corresponding Authors

Zhaoyi Li − *John A. Paulson School of Engineering and Applied Sciences, Harvard University, Cambridge, Massachusetts 02138, United States*; orcid.org/0000-0003-3661-8438; Email: zhaoyili@seas.harvard.edu

Federico Capasso − *John A. Paulson School of Engineering and Applied Sciences, Harvard University, Cambridge, Massachusetts 02138, United States*; Email: capasso@seas.harvard.edu

Authors

Raphaël Pestourie − *Department of Mathematics, Massachusetts Institute of Technology, Cambridge, Massachusetts 02139, United States*

https://doi.org/10.1021/acsphotonics.1c01850
ACS Photonics XXXX, XXX, XXX−XXX

Zin Lin − *Department of Mathematics, Massachusetts Institute of Technology, Cambridge, Massachusetts 02139, United States*

Steven G. Johnson − *Department of Mathematics, Massachusetts Institute of Technology, Cambridge, Massachusetts 02139, United States*

Complete contact information is available at: https://pubs.acs.org/10.1021/acsphotonics.1c01850

Notes

The authors declare no competing financial interest.

■ ACKNOWLEDGMENTS

Z. Li and F.C. acknowledge funding support through the Defense Advanced Research Projects Agency (Grant #HR00111810001). R.P., Z. Lin, and S.G.J. acknowledge funding support by the U.S. Army Research Office through the Institute for Soldier Nanotechnologies (Award #W911NF-18-2-0048). R.P. and Z. Lin were partially supported by the MIT-IBM Watson AI Laboratory (Challenge #2415).

■ REFERENCES

(1) Yu, N.; Capasso, F. Flat optics with designer metasurfaces. *Nat. Mater.* **2014**, *13*, 139−150.
(2) Chen, H.-T.; Taylor, A. J.; Yu, N. A review of metasurfaces: physics and applications. *Rep. Prog. Phys.* **2016**, *79*, 076401.
(3) He, Q.; Sun, S.; Xiao, S.; Zhou, L. High-efficiency metasurfaces: principles, realizations, and applications. *Adv. Opt. Mater.* **2018**, *6*, 1800415.
(4) Park, J.; Jeong, B. G.; Kim, S. I.; Lee, D.; Kim, J.; Shin, C.; Lee, C. B.; Otsuka, T.; Kyoung, J.; Kim, S.; et al. All-solid-state spatial light modulator with independent phase and amplitude control for three-dimensional LiDAR applications. *Nat. Nanotechnol.* **2021**, *16*, 69−76.
(5) Faraji-Dana, M.; Arbabi, E.; Arbabi, A.; Kamali, S. M.; Kwon, H.; Faraon, A. Compact folded metasurface spectrometer. *Nat. Commun.* **2018**, *9*, 1−8.
(6) Zhu, A. Y.; Chen, W. T.; Sisler, J.; Yousef, K. M.; Lee, E.; Huang, Y. W.; Qiu, C. W.; Capasso, F. Compact aberration-corrected spectrometers in the visible using dispersion-tailored metasurfaces. *Adv. Opt. Mater.* **2019**, *7*, 1801144.
(7) McClung, A.; Samudrala, S.; Torfeh, M.; Mansouree, M.; Arbabi, A. Snapshot spectral imaging with parallel metasystems. *Sci. Adv.* **2020**, *6*, eabc7646.
(8) Rubin, N. A.; D'Aversa, G.; Chevalier, P.; Shi, Z.; Chen, W. T.; Capasso, F. Matrix Fourier optics enables a compact full-Stokes polarization camera. *Science* **2019**, *365*, eaax1839.
(9) Lin, R. J.; Su, V.-C.; Wang, S.; Chen, M. K.; Chung, T. L.; Chen, Y. H.; Kuo, H. Y.; Chen, J.-W.; Chen, J.; Huang, Y.-T.; et al. Achromatic metalens array for full-colour light-field imaging. *Nat. Nanotechnol.* **2019**, *14*, 227−231.
(10) Guo, Q.; Shi, Z.; Huang, Y.-W.; Alexander, E.; Qiu, C.-W.; Capasso, F.; Zickler, T. Compact single-shot metalens depth sensors inspired by eyes of jumping spiders. *Proc. Natl. Acad. Sci. U. S. A.* **2019**, *116*, 22959−22965.
(11) Joo, W.-J.; Kyoung, J.; Esfandyarpour, M.; Lee, S.-H.; Koo, H.; Song, S.; Kwon, Y.-N.; Song, S. H.; Bae, J. C.; Jo, A.; et al. Metasurface-driven OLED displays beyond 10,000 pixels per inch. *Science* **2020**, *370*, 459−463.
(12) Lee, G.-Y.; Hong, J.-Y.; Hwang, S.; Moon, S.; Kang, H.; Jeon, S.; Kim, H.; Jeong, J.-H.; Lee, B. Metasurface eyepiece for augmented reality. *Nat. Commun.* **2018**, *9*, 1−10.
(13) Li, Z.; Lin, P.; Huang, Y.-W.; Park, J.-S.; Chen, W. T.; Shi, Z.; Qiu, C.-W.; Cheng, J.-X.; Capasso, F. Meta-optics achieves RGB-achromatic focusing for virtual reality. *Sci. Adv.* **2021**, *7*, eabe4458.
(14) Lalanne, P. Waveguiding in blazed-binary diffractive elements. *J. Opt. Soc. Am. A* **1999**, *16*, 2517−2520.
(15) Khorasaninejad, M.; Capasso, F. Broadband multifunctional efficient meta-gratings based on dielectric waveguide phase shifters. *Nano Lett.* **2015**, *15*, 6709−6715.
(16) Molesky, S.; Lin, Z.; Piggott, A. Y.; Jin, W.; Vucković, J.; Rodriguez, A. W. Inverse design in nanophotonics. *Nat. Photonics* **2018**, *12*, 659−670.
(17) Campbell, S. D.; Sell, D.; Jenkins, R. P.; Whiting, E. B.; Fan, J. A.; Werner, D. H. Review of numerical optimization techniques for meta-device design. *Opt. Mater. Express* **2019**, *9*, 1842−1863.
(18) Elsawy, M. M.; Lanteri, S.; Duvigneau, R.; Fan, J. A.; Genevet, P. Numerical optimization methods for metasurfaces. *Laser Photonics Rev.* **2020**, *14*, 1900445.
(19) Yao, K.; Unni, R.; Zheng, Y. Intelligent nanophotonics: merging photonics and artificial intelligence at the nanoscale. *Nanophotonics* **2019**, *8*, 339−366.
(20) Jiang, J.; Chen, M.; Fan, J. A. Deep neural networks for the evaluation and design of photonic devices. *Nat. Rev. Mater.* **2021**, *6*, 1−22.
(21) So, S.; Badloe, T.; Noh, J.; Bravo-Abad, J.; Rho, J. Deep learning enabled inverse design in nanophotonics. *Nanophotonics* **2020**, *9*, 1041−1057.
(22) Khatib, O.; Ren, S.; Malof, J.; Padilla, W. J. Deep Learning the Electromagnetic Properties of Metamaterials—A Comprehensive Review. *Adv. Funct. Mater.* **2021**, *31*, 2101748.
(23) Bendsoe, M. P.; Sigmund, O. *Topology Optimization: Theory, Methods, And Applications*; Springer Science & Business Media, 2013.
(24) Jensen, J. S.; Sigmund, O. Topology optimization for nano-photonics. *Laser Photonics Rev.* **2011**, *5*, 308−321.
(25) Sigmund, O. On the usefulness of non-gradient approaches in topology optimization. *Structural and Multidisciplinary Optimization* **2011**, *43*, 589−596.
(26) Miller, O. D. *Photonic Design: From Fundamental Solar Cell Physics to Computational Inverse Design*; University of California: Berkeley, 2012.
(27) Lalau-Keraly, C. M.; Bhargava, S.; Miller, O. D.; Yablonovitch, E. Adjoint shape optimization applied to electromagnetic design. *Opt. Express* **2013**, *21*, 21693−21701.
(28) Fan, J. A. Freeform metasurface design based on topology optimization. *MRS Bull.* **2020**, *45*, 196−201.
(29) Sell, D.; Yang, J.; Doshay, S.; Yang, R.; Fan, J. A. Large-angle, multifunctional metagratings based on freeform multimode geometries. *Nano Lett.* **2017**, *17*, 3752−3757.
(30) Xu, M.; Pu, M.; Sang, D.; Zheng, Y.; Li, X.; Ma, X.; Guo, Y.; Zhang, R.; Luo, X. Topology-optimized catenary-like metasurface for wide-angle and high-efficiency deflection: from a discrete to continuous geometric phase. *Opt. Express* **2021**, *29*, 10181−10191.
(31) Xiao, T. P.; Cifci, O. S.; Bhargava, S.; Chen, H.; Gissibl, T.; Zhou, W.; Giessen, H.; Toussaint, K. C., Jr; Yablonovitch, E.; Braun, P. V. Diffractive spectral-splitting optical element designed by adjoint-based electromagnetic optimization and fabricated by femtosecond 3D direct laser writing. *ACS Photonics* **2016**, *3*, 886−894.
(32) Sell, D.; Yang, J.; Doshay, S.; Fan, J. A. Periodic dielectric metasurfaces with high-efficiency, multiwavelength functionalities. *Adv. Opt. Mater.* **2017**, *5*, 1700645.
(33) Lin, Z.; Groever, B.; Capasso, F.; Rodriguez, A. W.; Lončar, M. Topology-optimized multilayered metaoptics. *Phys. Rev. Appl.* **2018**, *9*, 044030.
(34) Lin, Z.; Liu, V.; Pestourie, R.; Johnson, S. G. Topology optimization of freeform large-area metasurfaces. *Opt. Express* **2019**, *27*, 15765−15775.
(35) Callewaert, F.; Velev, V.; Kumar, P.; Sahakian, A.; Aydin, K. Inverse-designed broadband all-dielectric electromagnetic metadevices. *Sci. Rep.* **2018**, *8*, 1−8.
(36) Ballew, C.; Roberts, G.; Camayd-Muñoz, S.; Debbas, M. F.; Faraon, A. Mechanically reconfigurable multi-functional meta-optics studied at microwave frequencies. *Sci. Rep.* **2021**, *11*, 1−9.
(37) Christiansen, R. E.; Lin, Z.; Roques-Carmes, C.; Salamin, Y.; Kooi, S. E.; Joannopoulos, J. D.; Soljačić, M.; Johnson, S. G. Fullwave

Maxwell inverse design of axisymmetric, tunable, and multi-scale multi-wavelength metalenses. *Opt. Express* **2020**, *28*, 33854−33868.
(38) Shi, Z.; Zhu, A. Y.; Li, Z.; Huang, Y.-W.; Chen, W. T.; Qiu, C.-W.; Capasso, F. Continuous angle-tunable birefringence with freeform metasurfaces for arbitrary polarization conversion. *Sci. Adv.* **2020**, *6*, eaba3367.
(39) Phan, T.; Sell, D.; Wang, E. W.; Doshay, S.; Edee, K.; Yang, J.; Fan, J. A. High-efficiency, large-area, topology-optimized metasurfaces. *Light: Sci. Appl.* **2019**, *8*, 1−9.
(40) Lin, Z.; Johnson, S. G. Overlapping domains for topology optimization of large-area metasurfaces. *Opt. Express* **2019**, *27*, 32445−32453.
(41) Mansouree, M.; Kwon, H.; Arbabi, E.; McClung, A.; Faraon, A.; Arbabi, A. Multifunctional 2.5 D metastructures enabled by adjoint optimization. *Optica* **2020**, *7*, 77−84.
(42) Wang, E. W.; Sell, D.; Phan, T.; Fan, J. A. Robust design of topology-optimized metasurfaces. *Opt. Mater. Express* **2019**, *9*, 469−482.
(43) Zhou, M.; Lazarov, B. S.; Wang, F.; Sigmund, O. Minimum length scale in topology optimization by geometric constraints. *Computer Methods in Applied Mechanics and Engineering* **2015**, *293*, 266−282.
(44) Hammond, A. M.; Oskooi, A.; Johnson, S. G.; Ralph, S. E. Photonic topology optimization with semiconductor-foundry design-rule constraints. *Opt. Express* **2021**, *29*, 23916−23938.
(45) Cheeseman, P. C.; Kanefsky, B.; Taylor, W. M. In *Where the Really Hard Problems Are*; IJCAI, 1991; pp 331−337.
(46) Gershenfeld, N. A.; Gershenfeld, N. *The Nature of Mathematical Modeling*; Cambridge University Press, 1999.
(47) Martí, R. Multi-start methods. In *Handbook of Metaheuristics*; Springer, 2003; pp 355−368.
(48) Floudas, C. A. *Deterministic Global Optimization: Theory, Methods and Applications*; Springer Science & Business Media, 2013; Vol. *37*.
(49) Kuang, Z.; Miller, O. D. Computational bounds to light−matter interactions via local conservation laws. *Phys. Rev. Lett.* **2020**, *125*, 263607.
(50) Molesky, S.; Chao, P.; Rodriguez, A. W. Causality, Passivity and Optimization: Strong Duality in Quadratically Constrained Quadratic Programs for Waves. *arXiv*, May 5, 2021, 2105.02154v1. DOI: 10.48550/arXiv.2105.02154 (accessed on December 5, 2021).
(51) Angeris, G.; Vuckovic, J.; Boyd, S. P. Computational bounds for photonic design. *ACS Photonics* **2019**, *6*, 1232−1239.
(52) Gustafsson, M.; Schab, K.; Jelinek, L.; Capek, M. Upper bounds on absorption and scattering. *New J. Phys.* **2020**, *22*, 073013.
(53) Feichtner, T.; Selig, O.; Kiunke, M.; Hecht, B. Evolutionary optimization of optical antennas. *Phys. Rev. Lett.* **2012**, *109*, 127701.
(54) Sui, S.; Ma, H.; Wang, J.; Feng, M.; Pang, Y.; Xia, S.; Xu, Z.; Qu, S. Symmetry-based coding method and synthesis topology optimization design of ultra-wideband polarization conversion metasurfaces. *Appl. Phys. Lett.* **2016**, *109*, 014104.
(55) Cai, H.; Srinivasan, S.; Czaplewski, D. A.; Martinson, A. B.; Gosztola, D. J.; Stan, L.; Loeffler, T.; Sankaranarayanan, S. K.; López, D. Inverse design of metasurfaces with non-local interactions. *npj Comput. Mater.* **2020**, *6*, 1−8.
(56) Jafar-Zanjani, S.; Inampudi, S.; Mosallaei, H. Adaptive genetic algorithm for optical metasurfaces design. *Sci. Rep.* **2018**, *8*, 1−16.
(57) Li, Z.; Stan, L.; Czaplewski, D. A.; Yang, X.; Gao, J. Broadband infrared binary-pattern metasurface absorbers with micro-genetic algorithm optimization. *Opt. Lett.* **2019**, *44*, 114−117.
(58) Jin, Z.; Mei, S.; Chen, S.; Li, Y.; Zhang, C.; He, Y.; Yu, X.; Yu, C.; Yang, J. K.; Luk'yanchuk, B.; et al. Complex inverse design of meta-optics by segmented hierarchical evolutionary algorithm. *ACS Nano* **2019**, *13*, 821−829.
(59) Dorigo, M.; Gambardella, L. M. Ant colonies for the travelling salesman problem. *biosystems* **1997**, *43*, 73−81.
(60) Lewis, A.; Weis, G.; Randall, M.; Galehdar, A.; Thiel, D. In *Optimising Efficiency and Gain of Small Meander Line RFID Antennas Using Ant Colony System*; 2009 IEEE Congress on Evolutionary Computation; IEEE, 2009; pp 1486−1492.
(61) Kildishev, A. V.; Chettiar, U. K.; Liu, Z.; Shalaev, V. M.; Kwon, D.-H.; Bayraktar, Z.; Werner, D. H. Stochastic optimization of low-loss optical negative-index metamaterial. *J. Opt. Soc. Am. B* **2007**, *24*, A34−A39.
(62) Ong, J. R.; Chu, H. S.; Chen, V. H.; Zhu, A. Y.; Genevet, P. Freestanding dielectric nanohole array metasurface for mid-infrared wavelength applications. *Opt. Lett.* **2017**, *42*, 2639−2642.
(63) Elsawy, M. M.; Lanteri, S.; Duvigneau, R.; Brière, G.; Mohamed, M. S.; Genevet, P. Global optimization of metasurface designs using statistical learning methods. *Sci. Rep.* **2019**, *9*, 1−15.
(64) Nagar, J.; Campbell, S.; Werner, D. Apochromatic singlets enabled by metasurface-augmented GRIN lenses. *Optica* **2018**, *5*, 99−102.
(65) Zhao, C.; Zhang, J. Binary plasmonics: launching surface plasmon polaritons to a desired pattern. *Opt. Lett.* **2009**, *34*, 2417−2419.
(66) Azunre, P.; Jean, J.; Rotschild, C.; Bulovic, V.; Johnson, S. G.; Baldo, M. A. Guaranteed global optimization of thin-film optical systems. *New J. Phys.* **2019**, *21*, 073050.
(67) Panda, S. S.; Vyas, H. S.; Hegde, R. S. Robust inverse design of all-dielectric metasurface transmission-mode color filters. *Opt. Mater. Express* **2020**, *10*, 3145−3159.
(68) Black, J.; Hashimzade, N.; Myles, G. *A Dictionary of Economics*; Oxford University Press, 2012.
(69) Wiecha, P. R.; Arbouet, A.; Girard, C.; Lecestre, A.; Larrieu, G.; Paillard, V. Evolutionary multi-objective optimization of colour pixels based on dielectric nanoantennas. *Nat. Nanotechnol.* **2017**, *12*, 163−169.
(70) Zhu, D. Z.; Gregory, M. D.; Werner, P. L.; Werner, D. H. Fabrication and characterization of multiband polarization independent 3-D-printed frequency selective structures with ultrawide fields of view. *IEEE Trans. Antennas Propag* **2018**, *66*, 6096−6105.
(71) Zhu, D. Z.; Whiting, E. B.; Campbell, S. D.; Burckel, D. B.; Werner, D. H. Optimal high efficiency 3D plasmonic metasurface elements revealed by lazy ants. *ACS Photonics* **2019**, *6*, 2741−2748.
(72) Shalaginov, M. Y.; Campbell, S. D.; An, S.; Zhang, Y.; Ríos, C.; Whiting, E. B.; Wu, Y.; Kang, L.; Zheng, B.; Fowler, C.; et al. Design for quality: reconfigurable flat optics based on active metasurfaces. *Nanophotonics* **2020**, *9*, 3505−3534.
(73) Whiting, E. B.; Campbell, S. D.; Kang, L.; Werner, D. H. Meta-atom library generation via an efficient multi-objective shape optimization method. *Opt. Express* **2020**, *28*, 24229−24242.
(74) Sajedian, I.; Kim, J.; Rho, J. Finding the optical properties of plasmonic structures by image processing using a combination of convolutional neural networks and recurrent neural networks. *Microsyst. Nanoeng.* **2019**, *5*, 1−8.
(75) Inampudi, S.; Mosallaei, H. Neural network based design of metagratings. *Appl. Phys. Lett.* **2018**, *112*, 241102.
(76) Nadell, C. C.; Huang, B.; Malof, J. M.; Padilla, W. J. Deep learning for accelerated all-dielectric metasurface design. *Opt. Express* **2019**, *27*, 27523−27535.
(77) Zhelyeznyakov, M. V.; Brunton, S.; Majumdar, A. Deep learning to accelerate scatterer-to-field mapping for inverse design of dielectric metasurfaces. *ACS Photonics* **2021**, *8*, 481−488.
(78) Kiarashinejad, Y.; Abdollahramezani, S.; Adibi, A. Deep learning approach based on dimensionality reduction for designing electromagnetic nanostructures. *npj Comput. Mater.* **2020**, *6*, 1−12.
(79) Liu, Z.; Zhu, Z.; Cai, W. Topological encoding method for data-driven photonics inverse design. *Opt. Express* **2020**, *28*, 4825−4835.
(80) Zhang, C.; Jin, J.; Na, W.; Zhang, Q.-J.; Yu, M. Multivalued neural network inverse modeling and applications to microwave filters. *IEEE Trans. Microwave Theory Technol.* **2018**, *66*, 3781−3797.
(81) Lin, R.; Zhai, Y.; Xiong, C.; Li, X. Inverse design of plasmonic metasurfaces by convolutional neural network. *Opt. Lett.* **2020**, *45*, 1362−1365.

https://doi.org/10.1021/acsphotonics.1c01850
ACS Photonics XXXX, XXX, XXX−XXX

(82) Liu, D.; Tan, Y.; Khoram, E.; Yu, Z. Training deep neural networks for the inverse design of nanophotonic structures. *ACS Photonics* **2018**, *5*, 1365−1369.
(83) Malkiel, I.; Mrejen, M.; Nagler, A.; Arieli, U.; Wolf, L.; Suchowski, H. Plasmonic nanostructure design and characterization via deep learning. *Light: Sci. Appl.* **2018**, *7*, 1−8.
(84) Ma, W.; Cheng, F.; Liu, Y. Deep-learning-enabled on-demand design of chiral metamaterials. *ACS Nano* **2018**, *12*, 6326−6334.
(85) An, S.; Fowler, C.; Zheng, B.; Shalaginov, M. Y.; Tang, H.; Li, H.; Zhou, L.; Ding, J.; Agarwal, A. M.; Rivero-Baleine, C.; et al. A deep learning approach for objective-driven all-dielectric metasurface design. *ACS Photonics* **2019**, *6*, 3196−3207.
(86) Ma, W.; Cheng, F.; Xu, Y.; Wen, Q.; Liu, Y. Probabilistic representation and inverse design of metamaterials based on a deep generative model with semi-supervised learning strategy. *Adv. Mater.* **2019**, *31*, 1901111.
(87) Liu, Z.; Raju, L.; Zhu, D.; Cai, W. A hybrid strategy for the discovery and design of photonic structures. *IEEE Journal on Emerging and Selected Topics in Circuits and Systems* **2020**, *10*, 126−135.
(88) Liu, Z.; Zhu, D.; Rodrigues, S. P.; Lee, K.-T.; Cai, W. Generative model for the inverse design of metasurfaces. *Nano Lett.* **2018**, *18*, 6570−6576.
(89) An, S.; Zheng, B.; Shalaginov, M. Y.; Tang, H.; Li, H.; Zhou, L.; Ding, J.; Agarwal, A. M.; Rivero-Baleine, C.; Kang, M.; et al. Deep learning modeling approach for metasurfaces with high degrees of freedom. *Opt. Express* **2020**, *28*, 31932−31942.
(90) Jiang, J.; Sell, D.; Hoyer, S.; Hickey, J.; Yang, J.; Fan, J. A. Free-form diffractive metagrating design based on generative adversarial networks. *ACS Nano* **2019**, *13*, 8872−8878.
(91) Wen, F.; Jiang, J.; Fan, J. A. Robust freeform metasurface design based on progressively growing generative networks. *ACS Photonics* **2020**, *7*, 2098−2104.
(92) Kudyshev, Z. A.; Kildishev, A. V.; Shalaev, V. M.; Boltasseva, A. Machine-learning-assisted metasurface design for high-efficiency thermal emitter optimization. *Appl. Phys. Rev.* **2020**, *7*, 021407.
(93) Jiang, J.; Fan, J. A. Global optimization of dielectric metasurfaces using a physics-driven neural network. *Nano Lett.* **2019**, *19*, 5366−5372.
(94) Zimek, A.; Schubert, E.; Kriegel, H. P. A survey on unsupervised outlier detection in high-dimensional numerical data. *Statistical Analysis and Data Mining: The ASA Data Science Journal* **2012**, *5*, 363−387.
(95) Marimont, R. B.; Shapiro, M. B. Nearest neighbour searches and the curse of dimensionality. *J. Inst. Math. Its Appl.* **1979**, *24*, 59−70.
(96) Pestourie, R.; Mroueh, Y.; Nguyen, T. V.; Das, P.; Johnson, S. G. Active learning of deep surrogates for PDEs: application to metasurface design. *npj Comput. Mater.* **2020**, *6*, 1−7.
(97) Qu, Y.; Jing, L.; Shen, Y.; Qiu, M.; Soljacic, M. Migrating knowledge between physical scenarios based on artificial neural networks. *ACS Photonics* **2019**, *6*, 1168−1174.
(98) Chen, Y.; Lu, L.; Karniadakis, G. E.; Dal Negro, L. Physics-informed neural networks for inverse problems in nano-optics and metamaterials. *Opt. Express* **2020**, *28*, 11618−11633.
(99) Lu, L.; Pestourie, R.; Yao, W.; Wang, Z.; Verdugo, F.; Johnson, S. G. Physics-informed neural networks with hard constraints for inverse design. *SIAM Journal on Scientific Computing* **2021**, *43*, B1105−B1132.
(100) An, S.; Zheng, B.; Shalaginov, M. Y.; Tang, H.; Li, H.; Zhou, L.; Dong, Y.; Haerinia, M.; Agarwal, A. M.; Rivero-Baleine, C.; Kang, M.; Richardson, K. A.; Gu, T.; Hu, J.; Fowler, C.; Zhang, H. Deep Convolutional Neural Networks to Predict Mutual Coupling Effects in Metasurfaces. *Adv. Opt. Mater.* **2022**, *10*, 2102113.
(101) Pestourie, R.; Pérez-Arancibia, C.; Lin, Z.; Shin, W.; Capasso, F.; Johnson, S. G. Inverse design of large-area metasurfaces. *Opt. Express* **2018**, *26*, 33732−33747.
(102) Pérez-Arancibia, C.; Pestourie, R.; Johnson, S. G. Sideways adiabaticity: beyond ray optics for slowly varying metasurfaces. *Opt. Express* **2018**, *26*, 30202−30230.
(103) Hsu, L.; Dupré, M.; Ndao, A.; Yellowhair, J.; Kanté, B. Local phase method for designing and optimizing metasurface devices. *Opt. Express* **2017**, *25*, 24974−24982.
(104) Backer, A. S. Computational inverse design for cascaded systems of metasurface optics. *Opt. Express* **2019**, *27*, 30308−30331.
(105) Li, Z.; Pestourie, R.; Park, J.-S.; Huang, Y.-W.; Johnson, S. G.; Capasso, F. Inverse design enables large-scale high-performance meta-optics reshaping virtual reality. *Nat. Commun.* **2022**, *13*, 1−11.
(106) Bayati, E.; Pestourie, R.; Colburn, S.; Lin, Z.; Johnson, S. G.; Majumdar, A. Inverse designed extended depth of focus meta-optics for broadband imaging in the visible. *Nanophotonics* **2021**, DOI: 10.1515/nanoph-2021-0431.
(107) Pestourie, R.; Mroueh, Y.; Rackauckas, C.; Das, P.; Johnson, S.G. Physics-enhanced deep surrogates for PDEs. *arXiv*, Nov 10, **2021**, 2111.05841. (accessed on May 10, 2021).
(108) Skarda, J.; Trivedi, R.; Su, L.; Ahmad-Stein, D.; Kwon, H.; Han, S.; Fan, S.; Vučković, J. Low-overhead distribution strategy for simulation and optimization of large-area metasurfaces. *Computational Materials* **2022**, *8*, 1−6.
(109) Zhan, A.; Gibson, R.; Whitehead, J.; Smith, E.; Hendrickson, J. R.; Majumdar, A. Controlling three-dimensional optical fields via inverse Mie scattering. *Sci. Adv.* **2019**, *5*, eaax4769.
(110) Hughes, T. W.; Minkov, M.; Liu, V.; Yu, Z.; Fan, S. A perspective on the pathway toward full wave simulation of large area metalenses. *Appl. Phys. Lett.* **2021**, *119*, 150502.
(111) Lin, Z.; Roques-Carmes, C.; Pestourie, R.; Soljačić, M.; Majumdar, A.; Johnson, S. G. End-to-end nanophotonic inverse design for imaging and polarimetry. *Nanophotonics* **2021**, *10*, 1177−1187.
(112) Ng, A. Y. Feature selection, L 1 vs. L 2 regularization, and rotational invariance. In *Proceedings of the Twenty-First International Conference on Machine Learning*; Association for Computing Machinery, 2004; p 78.
(113) Tseng, E.; Colburn, S.; Whitehead, J.; Huang, L.; Baek, S.-H.; Majumdar, A.; Heide, F. Neural nano-optics for high-quality thin lens imaging. *Nat. Commun.* **2021**, *12*, 6493.
(114) Lin, X.; Rivenson, Y.; Yardimci, N. T.; Veli, M.; Luo, Y.; Jarrahi, M.; Ozcan, A. All-optical machine learning using diffractive deep neural networks. *Science* **2018**, *361*, 1004−1008.
(115) Thureja, P.; Shirmanesh, G. K.; Fountaine, K. T.; Sokhoyan, R.; Grajower, M.; Atwater, H. A. Array-level inverse design of beam steering active metasurfaces. *ACS Nano* **2020**, *14*, 15042−15055.
(116) Chung, H.; Miller, O. D. Tunable metasurface inverse design for 80% switching efficiencies and 144 angular deflection. *ACS Photonics* **2020**, *7*, 2236−2243.
(117) Hadibrata, W.; Wei, H.; Krishnaswamy, S.; Aydin, K. Inverse Design and 3D Printing of a Metalens on an Optical Fiber Tip for Direct Laser Lithography. *Nano Lett.* **2021**, *21*, 2422−2428.
(118) Li, L.; Ruan, H.; Liu, C.; Li, Y.; Shuang, Y.; Alù, A.; Qiu, C.-W.; Cui, T. J. Machine-learning reprogrammable metasurface imager. *Nat. Commun.* **2019**, *10*, 1−8.
(119) Spägele, C.; Tamagnone, M.; Kazakov, D.; Ossiander, M.; Piccardo, M.; Capasso, F. Multifunctional wide-angle optics and lasing based on supercell metasurfaces. *Nat. Commun.* **2021**, *12*, 1−10.
(120) Kosaka, H.; Kawashima, T.; Tomita, A.; Notomi, M.; Tamamura, T.; Sato, T.; Kawakami, S. Superprism phenomena in photonic crystals. *Phys. Rev. B* **1998**, *58*, R10096.
(121) Reshef, O.; DelMastro, M. P.; Bearne, K. K.; Alhulaymi, A. H.; Giner, L.; Boyd, R. W.; Lundeen, J. S. An optic to replace space and its application towards ultra-thin imaging systems. *Nat. Commun.* **2021**, *12*, 1−8.
(122) Gubbin, C. R.; De Liberato, S. Optical nonlocality in polar dielectrics. *Phys. Rev. X* **2020**, *10*, 021027.
(123) He, Q.; Sun, S.; Zhou, L. Tunable/reconfigurable metasurfaces: physics and applications. *Research* **2019**, *2019*, 1849272.
(124) Zheludev, N. I.; Plum, E. Reconfigurable nanomechanical photonic metamaterials. *Nat. Nanotechnol.* **2016**, *11*, 16−22.

https://doi.org/10.1021/acsphotonics.1c01850
ACS Photonics XXXX, XXX, XXX−XXX

(125) Nemati, A.; Wang, Q.; Hong, M.; Teng, J. Tunable and reconfigurable metasurfaces and metadevices. *Opto-Electron. Adv.* **2018**, *1*, 18000901.
(126) Shaltout, A. M.; Shalaev, V. M.; Brongersma, M. L. Spatiotemporal light control with active metasurfaces. *Science* **2019**, *364*, eaat3100.
(127) Lloyd, S. Enhanced sensitivity of photodetection via quantum illumination. *Science* **2008**, *321*, 1463−1465.
(128) Gregory, T.; Moreau, P.-A.; Toninelli, E.; Padgett, M. J. Imaging through noise with quantum illumination. *Sci. Adv.* **2020**, *6*, eaay2652.
(129) Tsang, M.; Nair, R.; Lu, X.-M. Quantum theory of superresolution for two incoherent optical point sources. *Phys. Rev. X* **2016**, *6*, 031033.
(130) Jha, P. K.; Ni, X.; Wu, C.; Wang, Y.; Zhang, X. Metasurface-enabled remote quantum interference. *Phys. Rev. Lett.* **2015**, *115*, 025501.
(131) Huang, T.; Zhao, X.; Zeng, S.; Crunteanu, A.; Shum, P. P.; Yu, N. Planar nonlinear metasurface optics and their applications. *Rep. Prog. Phys.* **2020**, *83*, 126101.
(132) Krasnok, A.; Tymchenko, M.; Alù, A. Nonlinear metasurfaces: a paradigm shift in nonlinear optics. *Mater. Today* **2018**, *21*, 8−21.
(133) Sain, B.; Meier, C.; Zentgraf, T. Nonlinear optics in all-dielectric nanoantennas and metasurfaces: a review. *Adv. Photonics* **2019**, *1*, 024002.
(134) Wang, C.; Li, Z.; Kim, M.-H.; Xiong, X.; Ren, X.-F.; Guo, G.-C.; Yu, N.; Lončar, M. Metasurface-assisted phase-matching-free second harmonic generation in lithium niobate waveguides. *Nat. Commun.* **2017**, *8*, 1−7.
(135) Sroor, H.; Huang, Y.-W.; Sephton, B.; Naidoo, D.; Valles, A.; Ginis, V.; Qiu, C.-W.; Ambrosio, A.; Capasso, F.; Forbes, A. High-purity orbital angular momentum states from a visible metasurface laser. *Nat. Photonics* **2020**, *14*, 498−503.
(136) Guo, X.; Ding, Y.; Duan, Y.; Ni, X. Nonreciprocal metasurface with space−time phase modulation. *Light: Sci. Appl.* **2019**, *8*, 1−9.
(137) Lawrence, M.; Barton, D. R., III; Dionne, J. A. Nonreciprocal flat optics with silicon metasurfaces. *Nano Lett.* **2018**, *18*, 1104−1109.

https://doi.org/10.1021/acsphotonics.1c01850
ACS Photonics XXXX, XXX, XXX−XXX